

Friction stir additive manufacturing enabling scale-up of ultrafine-grained pure copper with superior mechanical properties

M. Liu^{a,b}, B.B. Wang^b, X.H. An^c, P. Xue^{a,b,*}, F.C. Liu^b, L.H. Wu^{a,b}, D.R. Ni^{a,b,**}, B.L. Xiao^{a,b}, Z.Y. Ma^{a,b}

^a School of Materials Science and Engineering, University of Science and Technology of China, Shenyang, 110016, China

^b Shi-changxu Innovation Center for Advanced Materials, Institute of Metal Research, Chinese Academy of Sciences, 72 Wenhua Road, Shenyang, 110016, China

^c School of Aerospace, Mechanical and Mechatronic Engineering, The University of Sydney, Sydney, NSW, 2006, Australia

ARTICLE INFO

Keywords:

Friction stir additive manufacturing
Ultrafine-grained material
High strength
Microstructure
Copper

ABSTRACT

Bulk manufacturing has always been a big barrier to realize industrial application of ultrafine-grained (UFG) material for a long time. In this study, a new friction stir additive manufacturing (FSAM) method was developed, and three-dimensional large-scale bulk UFG pure Cu with uniform microstructure and high mechanical property was successfully manufactured.

1. Introduction

Over the last two decades, ultrafine-grained (UFG) materials have attracted extensive attention due to their remarkably enhanced strength and hardness compared to their coarse-grained (CG) counterparts [1,2]. It is well known that severe plastic deformation (SPD) methods can effectively produce the UFG metals and alloys through the sophisticated interactions of dislocation activities and twinning activities [3,4]. Among various SPD techniques [5], equal channel angular pressing (ECAP) and high-pressure torsion (HPT) have been widely used [6,7]. Although the high strength is readily obtained in UFG materials, the low ductility due to the limited dislocation activities in the fine grains and the serious cyclic softening during fatigue due to the microstructure instability are two critical concerns that restrict their application [1,8]. In addition, owing to the nature of SPD [2,9], it is difficult to enable the scale-up production of the UFG materials, becoming one of the most significant barriers to restricting their industrial applications [5].

Compared to the conventional SPD methods involving fundamental deformation mechanisms, the friction stir processing (FSP) technique that is based on the similar principle of friction stir welding (FSW) has been developed to produce remarkably uniform and stable UFG structure through the dynamic recrystallization (DRX) process [10]. The UFG

materials are characterized by the equiaxed grains with a large proportion of high angle grain boundaries (HAGBs) and low dislocation density [11,12]. These unique microstructural traits in UFG metals and alloys processed by FSP enabled the enhancement of tensile ductility and the improvement of cyclic softening [13]. Although large-area UFG materials can be prepared by multi-passes FSP [4], only the materials plate can be fabricated, and thereby it is still challenging to develop the three-dimensional large-scale UFG materials.

Nowadays, additive manufacturing (AM) has been recognized as a disruptive technology to produce materials through a layer-by-layer methodology [14]. In reality, the AM techniques can also be considered as a derivative of welding [15], indicating that there is theoretically no scale limit to produce materials via the pileup build mode between welds during the AM processing. Recently, based on the FSW, the novel friction stir additive manufacturing (FSAM) technology has been recently developed [15]. On the one hand, the coarser grains of the additive materials limit the mechanical properties improvement due to the high heat-input and thermal cyclic in the FSAM process [16]. On the other hand, owing to the nature of welding processes, there is usually a transitional zone (TZ) between two adjacent processed zones (PZs). The obvious softening in the heat-affected zone (HAZ) could lead to the significantly different microstructure and hardness between the TZ and

* Corresponding author. Shi-changxu Innovation Center for Advanced Materials, Institute of Metal Research, Chinese Academy of Sciences, 72 Wenhua Road, Shenyang 110016, China.

** Corresponding author. Shi-changxu Innovation Center for Advanced Materials, Institute of Metal Research, Chinese Academy of Sciences, 72 Wenhua Road, Shenyang 110016, China.

E-mail addresses: pxue@imr.ac.cn (P. Xue), dzni@imr.ac.cn (D.R. Ni).

<https://doi.org/10.1016/j.msea.2022.144088>

Received 30 May 2022; Received in revised form 21 September 2022; Accepted 22 September 2022

Available online 27 September 2022

0921-5093/© 2022 Elsevier B.V. All rights reserved.

the PZ, which will affect the overall mechanical properties of the bulk additive material [16,17]. Previous results have shown that the additional rapid cooling during the preparation of large-area bulk UFG pure copper by multi-pass FSP can effectively suppress the undesirable grain coarsening in HAZ and obtain the similar grain sizes in the TZ and PZ [18]. In this study, we select pure copper as a model material to explore the characteristics of the new FSAM processes, providing the basis for investigations of other complex materials. Herein, three-dimensional bulk pure Cu was fabricated by FSAM technique with rapid water cooling, and it is essential to systematically investigate the microstructures and mechanical properties. The aim is to obtain scale-up UFG Cu with uniform microstructures and excellent mechanical properties. Therefore, this work provides a novel FSAM technique can enable the scale-up production of full-dense UFG materials, which will not only advance our understanding of the structure-property relationship in UFG materials but also provide an exciting opportunity to prepare large-scale bulk UFG materials that will enrich and extend their potential engineering applications.

2. Experimental

Three-dimensional large-scale UFG pure Cu was prepared by employing the novel FSAM technique in this study. The base metal (BM) used in this study was conventional cold rolled commercially pure Cu (T3, 99.83 wt%). Numerous studies have shown that the microstructure of CR copper is inhomogeneous elongated grains with a high density of low angle grain boundaries (LAGBs) [19,20]. Cu sheet with a thickness of 2.8 mm was used as the base plate while other additive Cu sheets were 2 mm thick. Fig. 1a exhibits the schematic diagram of the FSAM process and the details of stir tool. Both the base plate and additive sheets were rigidly fixed in water in turn, and additively manufactured by eight-passes FSP with half of the pin diameter overlapping layer by layer along the same processing path and parameters on each plate. The FSP parameters have been optimized in our previous paper [21], thus, for each FSP process, the rotation rate, travel speed, tilt angle of the tool and

the plunge depth of the tool shoulder were 600 rpm, 50 mm/min, 3° and 0.2 mm, respectively, accompanied by additional rapid cooling with the flowing water to further reduce the heat input during FSAM process [22, 23].

Microstructural characterizations were performed by optical microscope (OM) and scanning electron microscopy (SEM) equipped with electron backscatter diffraction (EBSD). The specimens were machined by electro-discharge cutting perpendicular to the FSP direction. After grinding and mechanical polishing, OM specimens were corroded in a solution of 50 ml H₂O + 50 ml C₂H₅OH + 10 ml HCl + 8 g FeCl₃, and EBSD samples were electro-polished in a solution of 50 ml C₂H₅OH + 50 ml H₃PO₄ + 100 ml H₂O at room temperature at 5V for 60s.

Vickers microhardness followed the standard of ISO 6507-1: 2005 was measured along TZs and intermediate thickness of PZs on the cross-section of the FSAM sample under a load of 200 g for 15 s. As depicted by the dashed grid in the OM macrograph (Fig. 1b), measurements covering all intersections of the grid consisting of 16 columns and 11 rows were taken to exhibit the hardness distribution of the additive zone. Tensile test followed the standard of ISO 6892-1: 2019 was carried out along different FSAM directions and the specific sampling locations were shown in Fig. 1a. Dog-bone-shaped tensile specimens were prepared with a gauge length of 8 mm, a width of 3 mm and a thickness of ~9 mm along FSAM-Y direction, and a gauge length of 3 mm, a width of 1.4 mm and a thickness of ~0.5 mm along FSAM-Z direction, respectively. All the tensile tests were carried out at room temperature with an initial strain rate of $1 \times 10^{-3} \text{ s}^{-1}$. At least three tensile samples along each direction were tested to validate the reproducibility of the mechanical performance of the large three-dimensional bulk UFG Cu.

3. Results and discussion

As observed from Fig. 1b, the cross-section of the sample obtained after FSAM processing is composed of six-sheet layers with eight overlapped PZs in each layer, suggesting the formation of an effective large-area and defect-free bulk additive zone. The bright and dark contrasts

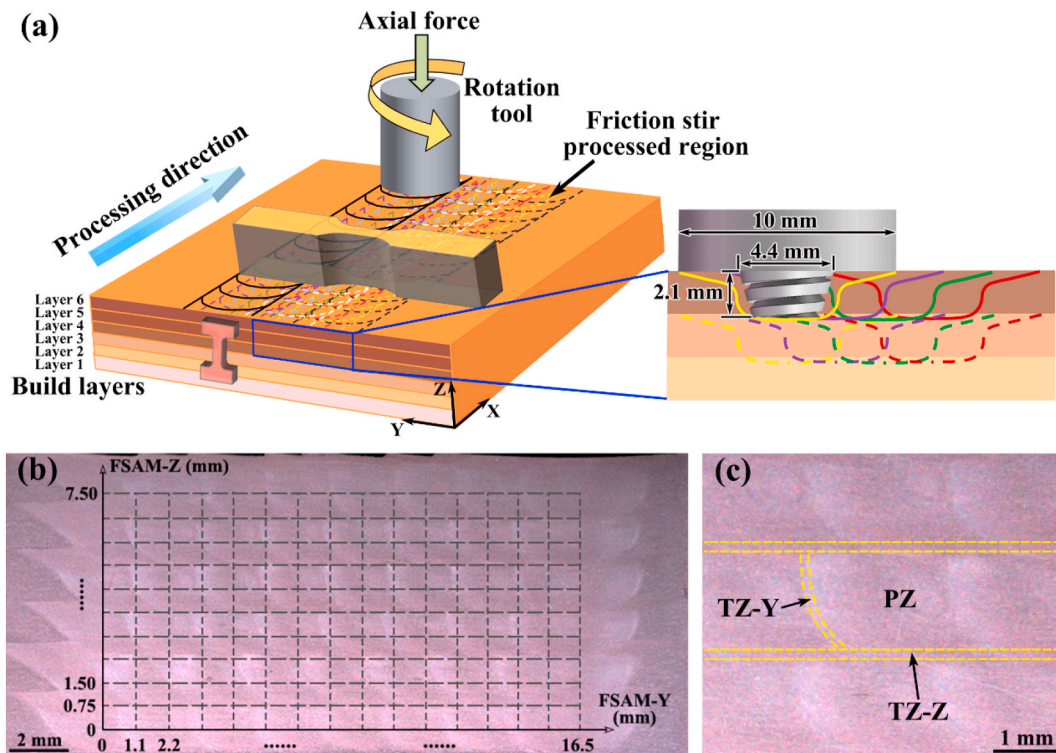


Fig. 1. (a) schematic diagram of FSAM process, (b) cross-sectional OM macrostructure with schematic of microhardness test (FSAM-Y indicates the direction perpendicular to FSP direction while FSAM-Z means the direction parallel to the additive direction) and (c) local magnification of the FSAM Cu sample.

throughout the cross-sectional OM macrostructure are stemmed from the recurrence of PZs and TZs, as shown in the high magnification OM image (Fig. 1c). It should be mentioned that the TZ-Z region was a transition zone distributed continuously between two additive plates, while the TZ-Y region was the transition zone between two adjacent PZs of multi-pass FSP and separated by TZ-Z layers.

Fig. 2 displays the microstructures in different regions of the FSAM Cu sample characterized by the EBSD technique. The inverse pole figure (IPF) maps in Fig. 2a–c shows that the equiaxed ultrafine grains were uniformly formed in both PZs and TZs, exhibiting the primary feature of the DRX structure, which is in line with that in FSP UFG materials [24–26]. The LAGBs ($2^\circ < \text{misorientation angle} < 15^\circ$) and HAGBs (misorientation angle $\geq 15^\circ$) were depicted by white and black lines, respectively.

It was proposed that the continuous DRX (CDRX) through restoration mechanisms dominated the microstructure evolution during FSW of pure Cu [27]. However, Mironov et al. had revealed that the DRX mechanism in FSW of pure copper was decided by the process temperature [28]. They indicated that the CDRX was the major mechanism at temperature below $0.5 T_m$ (T_m is the melting point), while discontinuous DRX (DDRDX) played a crucial role at temperature above $0.5 T_m$. Our previous work has proved that a significantly reduced heat input via additional rapid cooling during FSW of pure copper, making the peak temperature no more than $0.5 T_m$ [22]. Hence, it can be deduced that the CDRX might be the main mechanism of governing the grain structure formation in FSAM process. In addition, earlier study found that there was no obvious effect on the mechanical properties by the maximum pole density value of 8.83 [18,29]. The maximum pole density values in PZ, TZ-Y and TZ-Z regions were 3.00, 3.69 and 2.94, respectively. Therefore, the weak texture of the UFG Cu processed by FSP could have trivial effects on its static mechanical performance. The grain size

distributions in the regions of PZ, TZ-Y, and TZ-Z are quite similar and narrow, as revealed in Fig. 3, and the average grain sizes are ~ 450 nm, ~ 410 nm, and ~ 430 nm, respectively. Clearly, the grain sizes were quite larger than those obtained by ECAP [30] and HPT [31] due to the nature of the DRX structure. The relatively smaller grain size in TZs could be attributed to the lower temperature in the edge and bottom of the PZ during the overlapping FSP with flowing water cooling [16]. Moreover, compared to those of the PZ, the grains in the TZs were slightly elongated along with the longitudinal and transverse directions in the TZ-Y and TZ-Z regions, respectively. This mainly originated from the material flow around the PZ during FSP processes [32].

Based on the kernel average misorientation (KAM) maps reflecting the local misorientation shown in Fig. 2d–f, all the regions in the FSAM sample exhibits similar KAM distributions that are on the order of 0.32° , 0.30° , and 0.27° . It suggested that the low density of dislocations existed in these three FSAM regions, and most of them were more prone to be concentrated near the LAGBs because of the DRX process. Fig. 2g–i presents the distributions of grain boundary misorientation angle in PZ, TZ-Y, and TZ-Z regions, showing that the random distribution of cubic polycrystalline metals is achieved with high HAGBs fractions of 83.6%, 83.4%, and 82.7%, respectively. These values were much high than the fraction of $\sim 75\%$ of HAGBs and the fraction of $\sim 62\%$ of HAGB in Cu processed by 5 revolutions of HPT [31] and 24 passes of ECAP [33]. During the FSP processing, the DRX extensively occurred due to the nature of the high-temperature severe plastic deformation, and then the HAGB fractions of UFG Cu can be higher than $\sim 80\%$. In stark contrast, the conventional SPD methods, such as ECAP and HPT performed at room temperature, could not be able to provide sufficient driving forces to substantially activate the DRX processes, leading to the smaller grain sizes accompanied by a high density of LAGBs.

Previous investigations revealed that higher strain could be needed

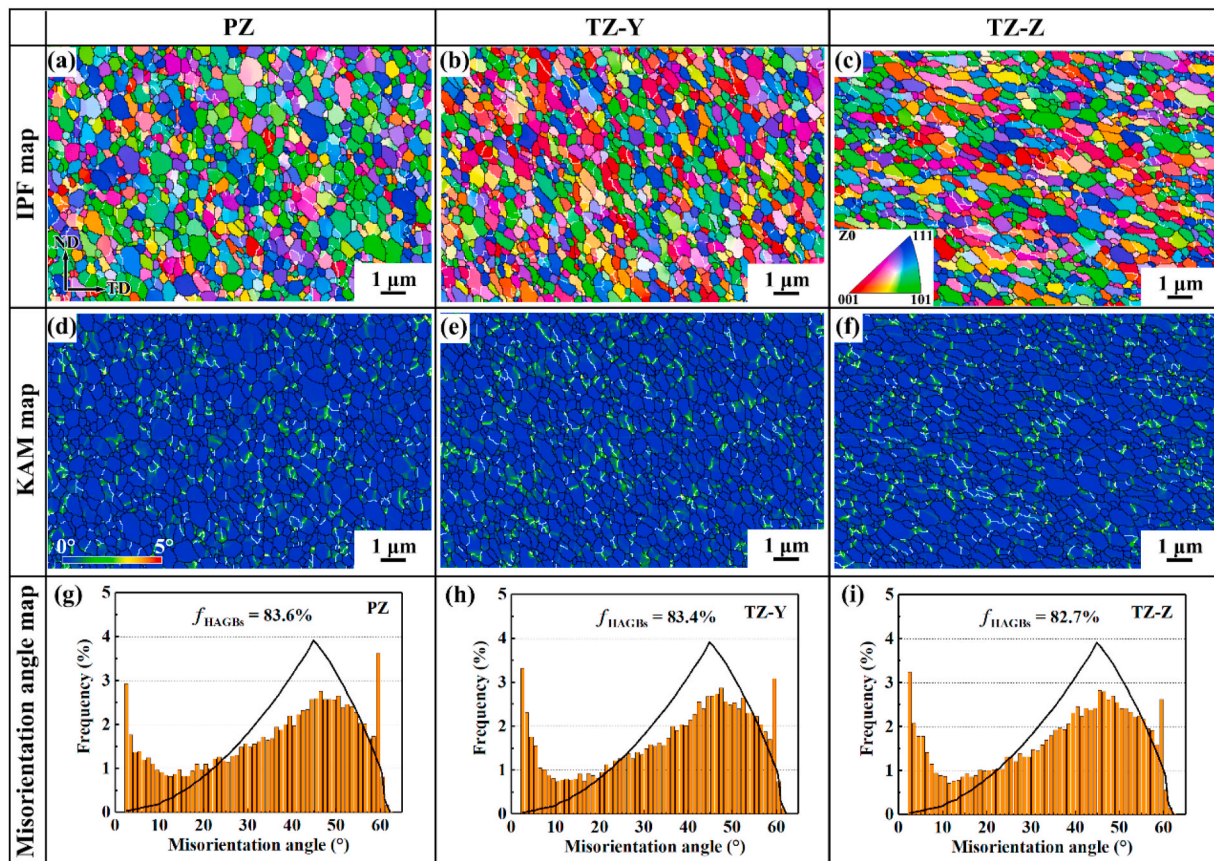


Fig. 2. EBSD microstructures of different regions in FSAM Cu sample: IPF maps of (a) PZ, (b) TZ-Y and (c) TZ-Z regions, KAM maps of (d) PZ, (e) TZ-Y and (f) TZ-Z regions, misorientation angle distribution maps of (g) PZ, (h) TZ-Y and (i) TZ-Z regions (TD: transverse direction, ND: normal direction).

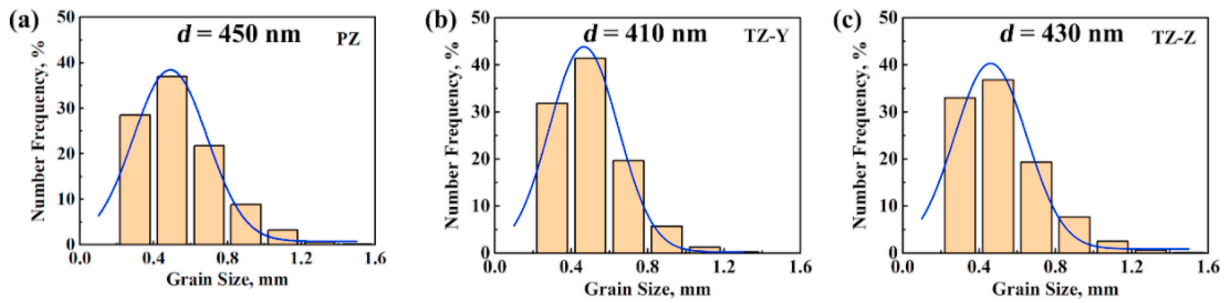


Fig. 3. Grain size distribution of FSAM samples: (a) PZ, (b) TZ-Y and (c) TZ-Z regions.

to obtain the homogeneous UFG structure in the materials with medium stacking fault energy (SFE) than those in the materials with high or low SFE [34]. This is because, for the materials with medium SFE, their dynamic recovery rates are relatively lower than that of high SFE materials and the formation of a homogeneously twinned structure is more difficult than that in low SFE materials, both of which are the rate-controlling mechanisms for the formation of UFG structures [4]. Herein, the homogeneous UFG microstructure in the FSAM Cu sample can be readily attained due to the DRX processes. Apart from the microstructural observations, the hardness measurements across the cross-section of the sample indicate a relatively uniform hardness distribution, as exhibited in Fig. 4a. The hardness test showed an average hardness value of 130.2 ± 1.4 HV for the BM. The average hardness value of the entire additive zone was 135.7 ± 5.6 HV, which was comparable to that of about 140 HV obtained by HPT [31], with all the hardness values ranging from 130.5 to 141.3 HV, no more than 5% variation in hardness. In detail, the typical microhardness line profiles are displayed in Fig. 4b. The PZ regions exhibited a low hardness value of 134.8 ± 1.6 HV while the hardness increased to 138.4 ± 1.8 HV in the

TZ areas, which could be correlated with the marginally reduced grain size in the TZ regions (Fig. 3).

Fig. 4c presents the typical tensile stress-strain curves of BM and UFG Cu specimens processed by FSAM, ECAP [35], and HPT [36], respectively. The yield strength of the initial BM was 271 ± 4 MPa. Although the grain sizes of the UFG Cu processed by FSAM were larger than those obtained by ECAP and HPT, the high yield strength of about 449 ± 7 MPa and 456 ± 1 MPa were obtained along with the FSAM-Y and FSAM-Z directions, respectively. These two values were even higher than that (385 MPa) obtained by 8-passes ECAP [35]. Recently, it was proposed that the Hall-Petch relationship for the fully recrystallized pure Cu can be divided into two stages [37]. When the average grain sizes are smaller than $3 \mu\text{m}$, the Hall-Petch slope in stage II is about 3 times that of the conventional one in stage I. Although the detailed mechanism is still unknown, the significantly higher K value suggests the extra hardening effect in the fine-grained and UFG regime with fully recrystallized microstructures. Considering the DRX processes in this study, based on the proposed equation of stage II ($\sigma_y = -123 + 347d^{-1/2}$, where σ_y is the yield strength and d is the average grain size

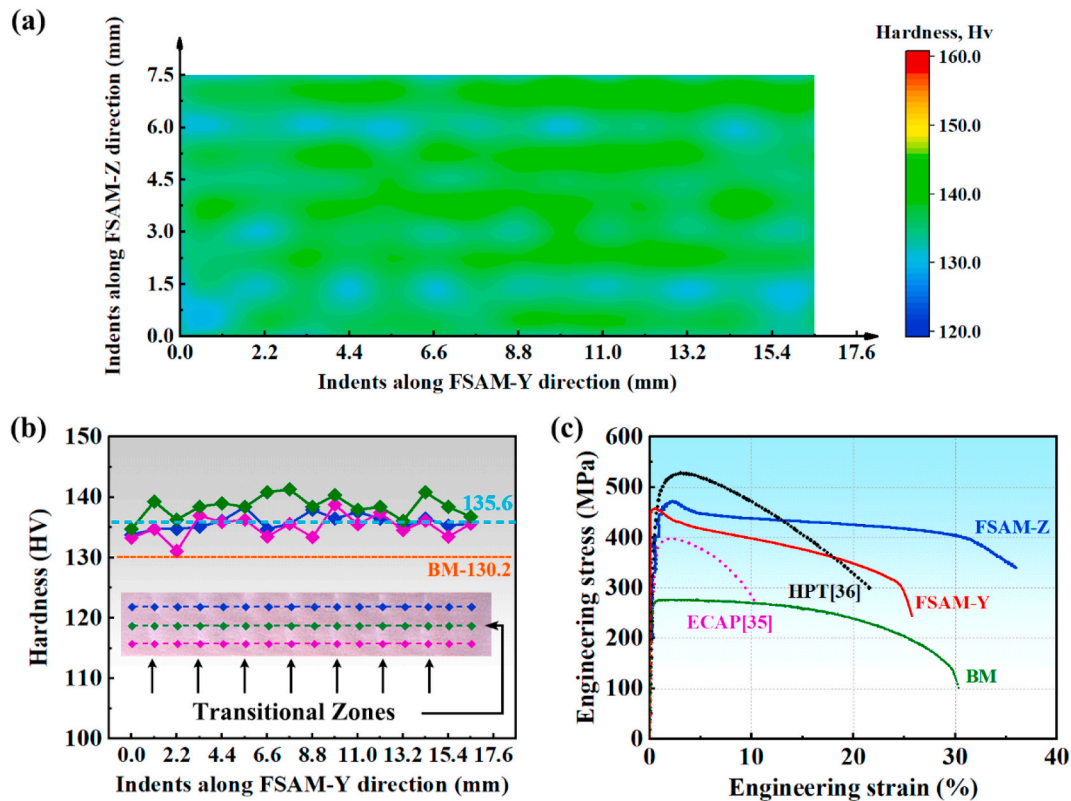


Fig. 4. Mechanical properties of FSAM Cu sample: (a) cross-sectional hardness distribution feature, (b) typical microhardness profiles along FSAM-Y direction, (c) engineering tensile stress-strain curves of UFG Cu processed by different SPD methods.

(μm) [37], the σ_y of the UFG Cu processed by FSAM was estimated to be about 420 MPa, which matched well with the experimental results.

It is well known that the plastic instability in terms of necking occurred quickly after the yielding in the UFG materials, leading to the undesirably low ductility, as demonstrated by the SPD samples [35,36]. In stark contrast, the very slow strain softening processes were prominently observed in the UFG Cu processed by FSAM specimens, indicating that the sudden plastic instability was greatly inhibited to delay the premature failure. This unique deformation feature rendered the UFG Cu by FSAM a better ductility compared to those obtained by conventional SPD methods, while the FSAM-Z direction specimens exhibited a slightly higher elongation of 32% than the FSAM-Y specimens (24%) due to the differences in sample sizes [38]. It indicated that the ductility of UFG materials could be effectively improved by introducing high-density twin boundaries, reducing dislocation density and increasing the proportion of HAGBs [39]. For FSP Cu, the unique equiaxed grains with high proportion of HAGBs, low density dislocations and weak texture were obtained [40]. In consequence, the ultrafine grains could effectively store dislocations during tensile deformation and the strain-hardening capacity could be improved, facilitating the acquisition of considerable ductility.

The fracture morphologies of the UFG specimens along FSAM-Y and FSAM-Z directions are exhibited in Fig. 5. For the FSAM-Y specimen in which the PZ and TZ-Z areas are under the iso-strain state, there are two distinct fracture morphologies that are derived from PZ and TZ-Z regions (Fig. 5a and b). The relatively deep and dense dimples covered the PZ areas, while the shallow dimples and several large voids were the typical fracture features in the TZ-Z regions. The TZ-Z region was susceptible to preferential failure during the tensile process owing to their different deformation capacities caused by the slight grain size differences between PZ and TZ-Z regions. Differently, for the FSAM-Z specimen in which PZ and TZ-Z regions are suffered from the same strain due to the iso-stress state, the localized deformation would readily occur in the PZ or PZ/TZ-Z interface (Fig. 5c and d).

It is well known that the hierarchically heterogeneous microstructures would be formed due to the fast heating and solidification processes enabled by other AM techniques such as selective laser melting (SLM) techniques [41,42]. In this study, the bulk UFG Cu with relatively homogeneous microstructures were successfully fabricated, exhibiting

higher strength than that (300 MPa) obtained by SLM [42], accompanied by good ductility. The attainment of the UFG microstructures can be attributed to the low rotation rate and the addition of water-cooling during the FSP process, rendering the remarkable reduction of the heat input to effectively suppress the grain coarsening in the TZ regions. More significantly, the FSAM method can readily enable the scale-up of the UFG microstructures and theoretically can produce the UFG samples with unlimited three-dimensional sizes, which will greatly extend and enrich the applications of the UFG materials.

4. Conclusion

In summary, the scale-up production of the full-dense UFG pure Cu was enabled by the use of the FSAM method. The bulk UFG pure Cu exhibited a roughly homogeneous DRX microstructure that enables the attainment of excellent mechanical properties. Regarding its effectiveness and efficiency, the FSAM method is readily applicable to a wide range of metal and alloy systems, opening up a new feasible avenue for the field of widely manufacturing large-scale bulk UFG materials.

CRediT authorship statement

M. Liu: Investigation, Formal analysis, Writing – original draft. **B.B. Wang:** Methodology, Formal analysis. **X.H. An:** Data curation, Writing – review & editing. **P. Xue:** Resources, Data curation, Writing – original draft, Writing – review & editing. **F.C. Liu:** Methodology, Formal analysis. **L.H. Wu:** Methodology, Formal analysis. **D.R. Ni:** Resources, Project administration, Data curation. **B.L. Xiao:** Supervision, Project administration. **Z.Y. Ma:** Project administration.

Originality statement

I write on behalf of myself and all co-authors to confirm that the results reported in the manuscript are original and neither the entire work, nor any of its parts have been previously published. The authors confirm that the article has not been submitted to peer review, nor has been accepted for publishing in another journal. The author(s) confirms that the research in their work is original, and that all the data given in the article are real and authentic. If necessary, the article can be

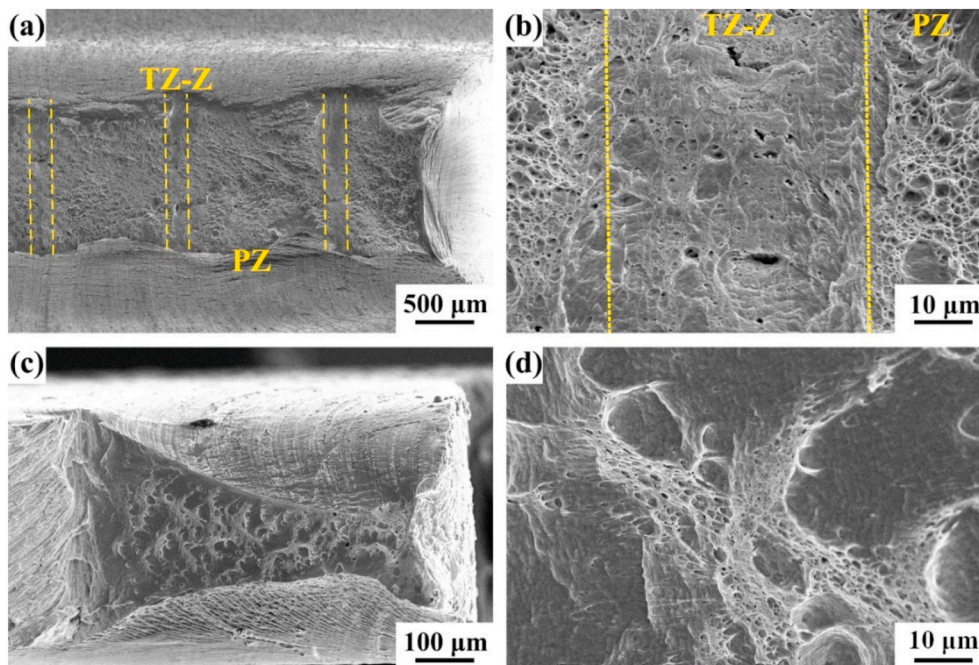


Fig. 5. Fractured morphologies of the UFG Cu specimens along (a), (b) FSAM-Y and (c), (d) FSAM-Z directions.

recalled, and errors corrected.

Declaration of competing interest

The authors declare that they have no known competing financial interests or personal relationships that could have appeared to influence the work reported in this paper.

Data availability

Data will be made available on request.

Acknowledgements

This work was supported by the National Natural Science Foundation of China under Grant No. 52071317, Liaoning Province Excellent Youth Foundation (2021-YQ-01), and the Youth Innovation Promotion Association of the Chinese Academy of Sciences (Y2021061). X.H. An acknowledges support from The University of Sydney under the Robinson Fellowship Scheme.

References

- [1] Y. Estrin, A. Vinogradov, Extreme grain refinement by severe plastic deformation: a wealth of challenging science, *Acta Mater.* 61 (3) (2013) 782–817.
- [2] Ruslan Z. Valiev, Yuri Estrin, Zenji Horita, Terence G. Langdon, Michael J. Zehetbauer, Y.T. Zhu, Producing bulk ultrafine-grained materials by severe plastic deformation, *JOM* 58 (2006) 33–39.
- [3] Y. Cao, S. Ni, X. Liao, M. Song, Y. Zhu, Structural evolutions of metallic materials processed by severe plastic deformation, *Mater. Sci. Eng. R Rep.* 133 (2018) 1–59.
- [4] X.H. An, S.D. Wu, Z.G. Wang, Z.F. Zhang, Significance of stacking fault energy in bulk nanostructured materials: insights from Cu and its binary alloys as model systems, *Prog. Mater. Sci.* 101 (2019) 1–45.
- [5] K. Edalati, A. Bachmaier, V.A. Beloshenko, Y. Beygelzimer, V.D. Blank, W.J. Botta, K. Bryla, J. Cízek, S. Divinski, N.A. Enikeev, Y. Estrin, G. Faraji, R.B. Figueiredo, M. Fujii, T. Furuta, T. Grosdidier, J. Gubicza, A. Hohenwarter, Z. Horita, J. Huot, Y. Ikoma, M. Janeček, M. Kawasaki, P. Král, S. Kuramoto, T.G. Langdon, D. R. Leiva, V.I. Levitas, A. Mazilkin, M. Mito, H. Miyamoto, T. Nishizaki, R. Pippan, V.V. Popov, E.N. Popova, G. Purcek, O. Renk, Á. Révész, X. Sauvage, V. Sklenicka, W. Skrotzki, B.B. Straumal, S. Suwas, L.S. Toth, N. Tsuji, R.Z. Valiev, G. Wilde, M. J. Zehetbauer, X. Zhu, Nanomaterials by severe plastic deformation: review of historical developments and recent advances, *Mater. Res. Lett.* 10 (4) (2022) 163–256.
- [6] R.Z. Valiev, T.G. Langdon, Principles of equal-channel angular pressing as a processing tool for grain refinement, *Prog. Mater. Sci.* 51 (7) (2006) 881–981.
- [7] A. Zhilyaev, T. Langdon, Using high-pressure torsion for metal processing: fundamentals and applications, *Prog. Mater. Sci.* 53 (6) (2008) 893–979.
- [8] X.H. An, S.D. Wu, Z.G. Wang, Z.F. Zhang, Enhanced cyclic deformation responses of ultrafine-grained Cu and nanocrystalline Cu–Al alloys, *Acta Mater.* 74 (2014) 200–214.
- [9] E. Bruder, Formability of ultrafine grained metals produced by severe plastic deformation—an overview, *Adv. Eng. Mater.* 21 (1) (2019) 180–316.
- [10] G.K. Padhy, C.S. Wu, S. Gao, Friction stir based welding and processing technologies - processes, parameters, microstructures and applications: a review, *J. Mater. Sci. Technol.* 34 (1) (2018) 1–38.
- [11] S. Palanivel, P. Nelaturu, B. Glass, R.S. Mishra, Friction stir additive manufacturing for high structural performance through microstructural control in an Mg based WE43 alloy, *Mater. Des.* 65 (1980–2015) 934–952, 2015.
- [12] X. Feng, H. Liu, S. Suresh Babu, Effect of grain size refinement and precipitation reactions on strengthening in friction stir processed Al–Cu alloys, *Scripta Mater.* 65 (12) (2011) 1057–1060.
- [13] P. Xue, B.B. Wang, X.H. An, D.R. Ni, B.L. Xiao, Z.Y. Ma, Improved cyclic softening behavior of ultrafine-grained Cu with high microstructural stability, *Scripta Mater.* 166 (2019) 10–14.
- [14] T. DebRoy, H.L. Wei, J.S. Zuback, T. Mukherjee, J.W. Elmer, J.O. Milewski, A. M. Beese, A. Wilson-Heid, A. De, W. Zhang, Additive manufacturing of metallic components – process, structure and properties, *Prog. Mater. Sci.* 92 (2018) 112–224.
- [15] A. Kumar Srivastava, N. Kumar, A. Rai Dixit, Friction stir additive manufacturing – an innovative tool to enhance mechanical and microstructural properties, *Mater. Sci. Eng., B* 263 (2021) 1–25.
- [16] C. He, Y. Li, Z. Zhang, J. Wei, X. Zhao, Investigation on microstructural evolution and property variation along building direction in friction stir additive manufactured Al–Zn–Mg alloy, *Mater. Sci. Eng., A* 777 (2020) 1–13.
- [17] Z.Y. Ma, S.R. Sharma, R.S. Mishra, Effect of multiple-pass friction stir processing on microstructure and tensile properties of a cast aluminum–silicon alloy, *Scripta Mater.* 54 (9) (2006) 1623–1626.
- [18] P. Xue, B.L. Xiao, Z.Y. Ma, Achieving large-area bulk ultrafine grained Cu via submerged multiple-pass friction stir processing, *J. Mater. Sci. Technol.* 29 (12) (2013) 1111–1115.
- [19] Z.N. Mao, R.C. Gu, F. Liu, Y. Liu, X.Z. Liao, J.T. Wang, Effect of equal channel angular pressing on the thermal-annealing-induced microstructure and texture evolution of cold-rolled copper, *Mater. Sci. Eng., A* 674 (2016) 186–192.
- [20] M. Xie, W. Huang, H. Chen, L. Gong, W. Xie, H. Wang, B. Yang, Microstructural evolution and strengthening mechanisms in cold-rolled Cu–Ag alloys, *J. Alloys Compd.* 851 (2021).
- [21] P. Xue, B.L. Xiao, Z.Y. Ma, High tensile ductility via enhanced strain hardening in ultrafine-grained Cu, *Mater. Sci. Eng., A* 532 (2012) 106–110.
- [22] P. Xue, B.L. Xiao, Q. Zhang, Z.Y. Ma, Achieving friction stir welded pure copper joints with nearly equal strength to the parent metal via additional rapid cooling, *Scripta Mater.* 64 (11) (2011) 1051–1054.
- [23] M.A. Wahid, Z.A. Khan, A.N. Siddiquee, Review on underwater friction stir welding: a variant of friction stir welding with great potential of improving joint properties, *Trans. Nonferrous Metals Soc. China* 28 (2) (2018) 193–219.
- [24] B.B. Wang, L.H. Wu, P. Xue, D.R. Ni, B.L. Xiao, Y.D. Liu, Z.Y. Ma, Improved high cycle fatigue property of ultrafine grained pure aluminum, *Mater. Lett.* (2020) 1–4.
- [25] Y. Wang, R. Fu, Y. Li, L. Zhao, A high strength and high electrical conductivity Cu–Cr–Zr alloy fabricated by cryogenic friction stir processing and subsequent annealing treatment, *Mater. Sci. Eng., A* 755 (2019) 166–169.
- [26] Y. Wang, R. Fu, L. Jing, D. Sang, Y. Li, Tensile behaviors of pure copper with different fraction of nonequilibrium grain boundaries, *Mater. Sci. Eng., A* 724 (2018) 164–170.
- [27] A. Heidarzadeh, T. Saeid, V. Klemm, A. Chabok, Y. Pei, Effect of stacking fault energy on the restoration mechanisms and mechanical properties of friction stir welded copper alloys, *Mater. Des.* 162 (2019) 185–197.
- [28] S. Mironov, K. Inagaki, Y.S. Sato, H. Kokawa, Microstructural evolution of pure copper during friction-stir welding, *Phil. Mag.* 95 (4) (2015) 367–381.
- [29] Y.D. Wang, M. Liu, B.H. Yu, L.H. Wu, P. Xue, D.R. Ni, Z.Y. Ma, Enhanced combination of mechanical properties and electrical conductivity of a hard state Cu–Cr–Zr alloy via one-step friction stir processing, *J. Mater. Process. Technol.* 288 (2021).
- [30] A. Mishra, B. Kad, F. Gregori, M. Meyers, Microstructural evolution in copper subjected to severe plastic deformation: experiments and analysis, *Acta Mater.* 55 (1) (2007) 13–28.
- [31] X.H. An, S.D. Wu, Z.F. Zhang, R.B. Figueiredo, N. Gao, T.G. Langdon, Evolution of microstructural homogeneity in copper processed by high-pressure torsion, *Scripta Mater.* 63 (5) (2010) 560–563.
- [32] H. Su, J. Chen, C. Wu, Effect of tool eccentricity on the periodic material flow in friction stir welding process, *Int. J. Mech. Sci.* 220 (2022).
- [33] C.X. Huang, H.J. Yang, S.D. Wu, Z.F. Zhang, Microstructural characterizations of Cu processed by ECAP from 4 to 24 passes, *Mater. Sci. Forum* 584–586 (2008) 333–337.
- [34] X.H. An, Q.Y. Lin, S.D. Wu, Z.F. Zhang, R.B. Figueiredo, N. Gao, T.G. Langdon, Significance of stacking fault energy on microstructural evolution in Cu and Cu–Al alloys processed by high-pressure torsion, *Phil. Mag.* 91 (25) (2011) 3307–3326.
- [35] F. Dalla Torre, R. Lapovok, J. Sandlin, P.F. Thomson, C.H.J. Davies, E.V. Pereloma, Microstructures and properties of copper processed by equal channel angular extrusion for 1–16 passes, *Acta Mater.* 52 (16) (2004) 4819–4832.
- [36] X.H. An, S.D. Wu, Z.F. Zhang, R.B. Figueiredo, N. Gao, T.G. Langdon, Enhanced strength–ductility synergy in nanostructured Cu and Cu–Al alloys processed by high-pressure torsion and subsequent annealing, *Scripta Mater.* 66 (5) (2012) 227–230.
- [37] Y.Z. Tian, Y.P. Ren, S. Gao, R.X. Zheng, J.H. Wang, H.C. Pan, Z.F. Zhang, N. Tsuji, G.W. Qin, Two-stage Hall–Petch relationship in Cu with recrystallized structure, *J. Mater. Sci. Technol.* 48 (2020) 31–35.
- [38] Y. Zhao, Y. Guo, Q. Wei, A. Dangelewicz, C. Xu, Y. Zhu, T. Langdon, Y. Zhou, E. Lavernia, Influence of specimen dimensions on the tensile behavior of ultrafine-grained Cu, *Scripta Mater.* 59 (6) (2008) 627–630.
- [39] Y. Zhao, Y. Zhu, E.J. Lavernia, Strategies for improving tensile ductility of bulk nanostructured materials, *Adv. Eng. Mater.* 12 (8) (2010) 769–778.
- [40] P. Xue, B.B. Wang, F.F. Chen, W.G. Wang, B.L. Xiao, Z.Y. Ma, Microstructure and mechanical properties of friction stir processed Cu with an ideal ultrafine-grained structure, *Mater. Char.* 121 (2016) 187–194.
- [41] Z.G. Zhu, Q.B. Nguyen, F.L. Ng, X.H. An, X.Z. Liao, P.K. Liaw, S.M.L. Nai, J. Wei, Hierarchical microstructure and strengthening mechanisms of a CoCrFeNiMn high entropy alloy additively manufactured by selective laser melting, *Scripta Mater.* 154 (2018) 20–24.
- [42] Z. Li, Y. Cui, W. Yan, D. Zhang, Y. Fang, Y. Chen, Q. Yu, G. Wang, H. Ouyang, C. Fan, Q. Guo, D.-B. Xiong, S. Jin, G. Sha, N. Ghoniem, Z. Zhang, Y.M. Wang, Enhanced strengthening and hardening via self-stabilized dislocation network in additively manufactured metals, *Mater. Today* 50 (2021) 79–88.